

Scanning Electron Microscopy of Experimental *Trichophyton mentagrophytes* Infections in Guinea Pig Skin

ROBERT D. HUTTON,* SHARON KERBS, AND KEN YEE

Department of Dermatology Research, Letterman Army Institute of Research, Presidio of San Francisco, San Francisco, California 94129

Received for publication 28 April 1978

Trichophyton mentagrophytes invasion of guinea pig skin was examined by scanning electron microscopy. Biopsies were obtained daily for 12 days from experimental infection sites. Dermatophyte invasion, examined in detail by scanning electron microscopy of cross-sectioned, prefixed skin was evidenced by: the appearance of hyphae within the stratum corneum; follicular invasion by hyphae, which remained initially within the follicle wall; emergence of the hyphae from the wall into the follicular canal; proliferation of the fungus down the follicle, with furrowing of the follicle wall and hair shaft cuticle; penetration of hyphae into the hair shaft by subcuticular and transcucicular routes; and massive peripilar hyphal proliferation with arthrosporangogenesis. A three-dimensional perception of the invasion sequence of a dermatophyte in guinea pig skin was obtained by scanning electron microscopy.

The intricate invasion pattern of dermatophytes in skin was carefully examined by light microscopy in 1955 (6). In the past few years, the scanning electron microscope (SEM) has greatly enhanced microstructural perceptions of biological and other materials. This paper presents a comprehensive SEM study of *Trichophyton mentagrophytes* invasion in guinea pig skin. Images which clearly demonstrate in vivo parasitic activities of this dermatophyte were achieved by SEM examination of prefixed, cross-sectioned lesion biopsies—a novel application of standard techniques which is described in this report.

Normal microanatomy of the skin has been previously described (6-8). Several microanatomic features were demonstrated for the first time in three-dimensional perspective by our techniques. These features, essential to interpretation of the micrographs, are described in Results.

MATERIALS AND METHODS

Animals. Infections were induced on the backs of 36 individually caged Chase-Moen guinea pigs of either sex. The outbred animals were raised in a closed breeding colony at our institute and weighed between 250 and 500 g.

Organisms. Microconidial inocula were made from cultures of *T. mentagrophytes* var. *granulosum* ATCC 18748 by the method of Reinhardt et al. (9), except Tween 40 was omitted. The concentration of viable spores in the preparation was determined by triplicate plate counts of 10-fold dilutions in sterile distilled water.

Infection procedure. Infections were induced according to the following standardized nonoccluded method of S. Kerbs et al. (manuscript in preparation). Animal backs were sheared with an Oster clipper (no. 40 blade attachment). One million viable microconidia in 25 μ l of sterile water were placed on the right midback of each animal and spread gently over a 1-cm² area with the tapered side of a micropipette. Twenty-five microliters of sterile water was similarly spread on the left midback of each animal as a control site.

Biopsies. Three guinea pigs were used daily for 12 consecutive days after spore inoculation. Before sacrifice, anesthetized animals underwent a wide-margined, full-thickness excisional biopsy of each inoculated site. Control sites were similarly biopsied on days 1, 5, and 12. The excised skin contracted on removal but was restored to original diameter before fixation by pinning the edges to a flat block of wax. Between the bottom of the biopsy and the wax was a sheet of filter paper to facilitate fixation of the underside.

The specimens were fixed overnight in 2% paraformaldehyde-2.5% glutaraldehyde in 0.1 M cacodylate buffer adjusted to pH 7.4. After being washed in 5% sucrose in cacodylate buffer, the specimens were cut from the center to the edge with clean single-edge razor blades into 1-mm-wide strips. Postfixing was done in 1% OsO₄, Zetterqvist salt solution (5) for 1 h. The specimens were dehydrated via a graded series of 25, 50, 75, 95, and 100% acetone. The acetone was displaced with carbon dioxide, and the tissues were critical-point dried in a Denton DCP-1 apparatus. After coating them with successive layers of carbon, silver, and gold in a Denton DV-502 vacuum evaporator equipped with rotating stage, all specimens were examined in an ETEC Autoscan electron microscope operated at 10 kV. Micrographs of skin surface and sectioned skin were recorded on Polaroid PN55 film.

RESULTS

Skin surface. The surface of the stratum corneum was virtually obscured by hair, even though the hair was closely clipped; no spores or hyphae were noted on the stratum corneum. A few surface hairs showed adherent, round, 2- to 3- μ m-diameter microconidia (Fig. 1).

Stratum corneum. Scanning of tissue surfaces exposed by sectioning showed hyphae both in the stratum corneum and in follicles from day 5 on. Figure 2 shows hyphae lying in smooth, compressed grooves in the lower stratum corneum, apparently between cell layers. However, it was not possible by our techniques to ascertain whether hyphae were intercellular or intracellular in the stratum corneum.

Early follicular invasion. Figures 3 and 4 depict the contiguous upper and lower portions of a longitudinally split hair follicle which is devoid of a hair shaft. These figures demonstrate several aspects of follicular anatomy seen by SEM. The follicular walls are composed of two sheaths, the inner and outer root sheaths. An inner root sheath is seen in Fig. 4; the cuticle is the innermost layer, made of overlapping flat cells with their free edges pointing downward. The surrounding layers of the inner root sheath (Huxley's and Henle's) were not discernible in this study. The inner root sheath is a keratinous structure which grows upward from the bottom of the follicle and glides over the stationary outer root sheath (8). Disintegration of the inner root sheath occurs (Fig. 3, lower right, and Fig. 4, upper left) near the level of sebaceous gland entry. Above this level (Fig. 3) the follicular wall

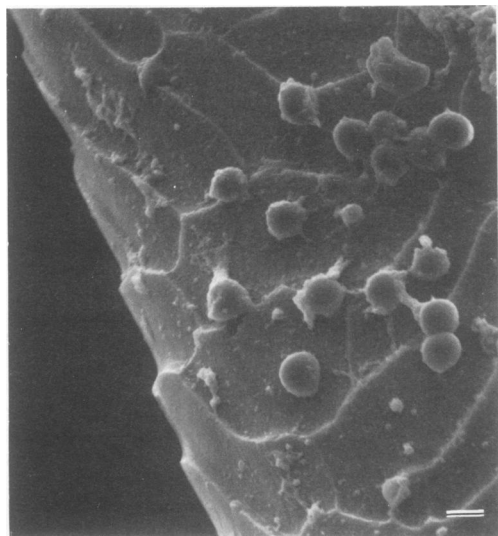


FIG. 1. Microconidia adherent to guinea pig hair shaft *in vivo*. Bar, 3 μ m.

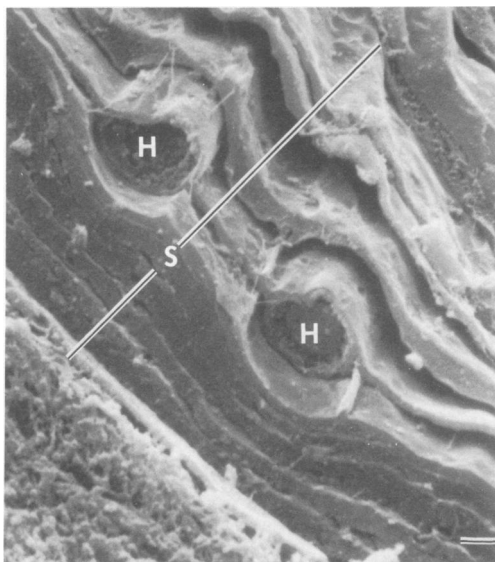


FIG. 2. Early hyphal (H) invasion of the stratum corneum (S), apparent pressuring between laminae. Bar, 0.75 μ m.

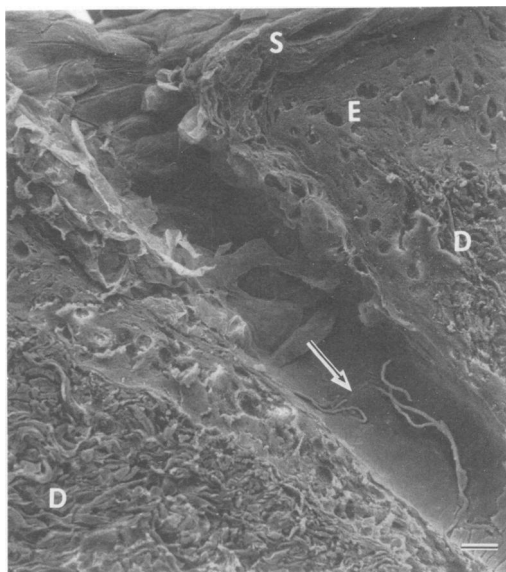


FIG. 3. Upper portion of follicle (devoid of hair shaft), emergence of hyphae into follicular canal (arrow). Note dermal collagen (D), epidermis (E), and stratum corneum (S). Bar, 15.9 μ m.

is all outer root sheath. The outer root sheath runs the length of the follicle but forms a keratinous lining only in the upper portion, where it is not lined by inner root sheath.

Figures 3 and 5 show features typical of a newly infected follicle. Hyphae were not visual-

ized in the upper portion of the follicular canal (Fig. 3). The early downward progress of the fungus apparently occurs within the outer root sheath. Hyphae were seen emerging from the lower region of the outer root sheath (Fig. 3, lower right). A higher magnification of this region is seen in Fig. 5. The fungus had, appar-

ently, not yet invaded the lower portion of the follicle (Fig. 4).

Peripilar proliferation. In normal skin, the peripilar region between the hair shaft and follicle wall is a potential space. In this space fungus may proliferate. Figure 6 demonstrates peripilar hyphal proliferation downward between the cuticle of the inner root sheath and its apposed hair shaft (absent here). Hyphae created furrows of various depths in follicular walls (Fig. 7) and hair shafts (Fig. 8).

Invasion of hair shaft. Hair shafts are composed of a cortex encased in a cuticle. Cuticular cells of the hair shaft are flat and overlapping, like the cuticular cells of the inner root sheath, but the free edges of the cells on the hair point upward. Hair shaft invasion may occur as hyphae wedge under the free edges of overlapping cuticular cells (Fig. 9) or, apparently, may occur by direct penetration through the cuticular cells (Fig. 10). Evidence of extensive hyphal tunneling beneath the cuticle of the hair shaft and of boring through the hair cortex can be seen in Fig. 11.

Arthrospore formation. Above the diagonally oriented hair shaft in Fig. 12, the wall of the longitudinally split follicle has been deflected into the plane of the photograph. The upper left region shows arthrospores forming from hyphae. The lower region of the wall above the hair shows spheroid arthrospores cupped in indentations of the wall's inner surface. The longitudinally split hair shown in Fig. 13 is surrounded

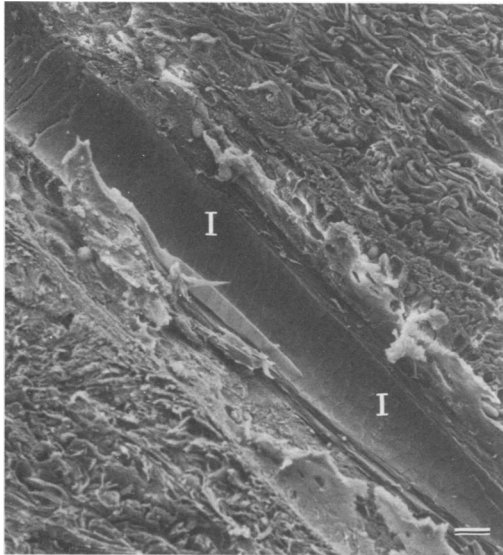


FIG. 4. Uninvaded contiguous lower part of follicle in Fig. 3. Note downward-pointing overlapped cells of inner root sheath cuticle (I). Disintegration of inner root sheath at upper left is normal. Bar, 15.9 μ m.

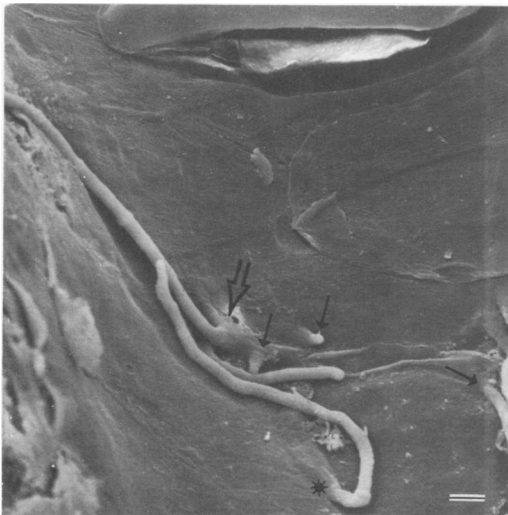


FIG. 5. Details of area lower left of arrow in Fig. 3. Note emergence of hyphae (small arrows), an apparent reentry into the wall (large arrow), and an aberrant, upward-pointing hypha (*). Bar, 2.9 μ m.

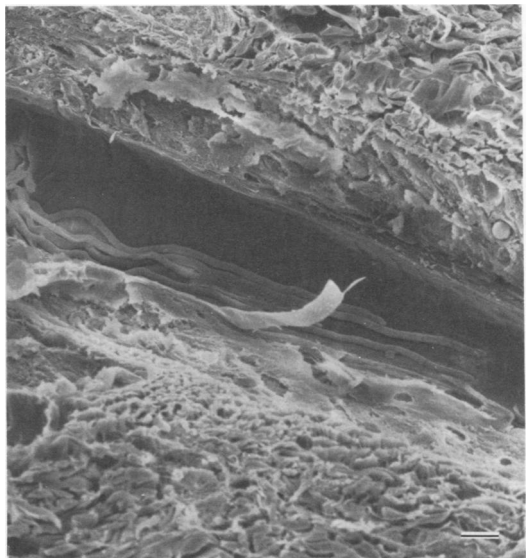


FIG. 6. Invasion of lower follicle, hyphae pressed against the cuticle of the inner root sheath. Bar, 10.5 μ m.

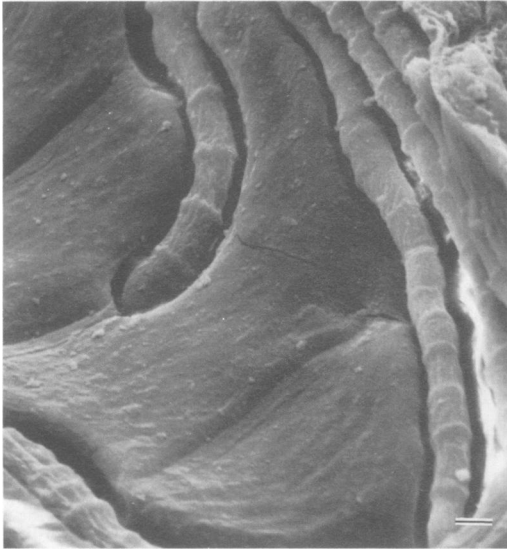


FIG. 7. Hyphal furrowing of the inner root sheath cuticle. Bar, 1.1 μ m.

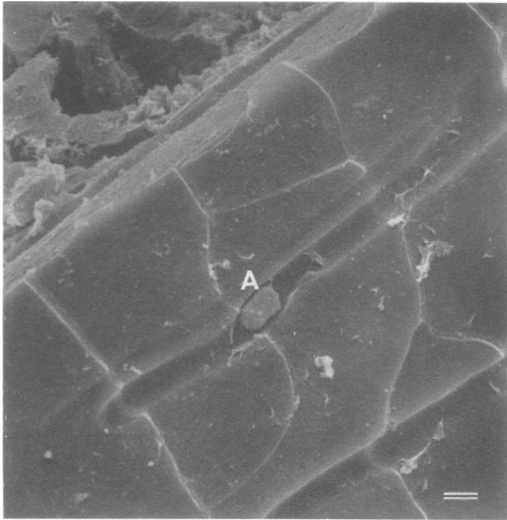


FIG. 8. Hair shaft surface with cuticular hyphal furrows and one retained arthrospore (A). Bar, 1.9 μ m.

by abundant arthrospores. Cortical tunnels resembled wormholes in wood. Figure 14 indicates the predominance of arthrospores in the peripilar region rather than in the hair shaft and also illustrates the smoothly carved nature of cortical tunnels. Figure 15 shows a cross-sectioned follicle. Sandwiched between the follicular wall and the hair (itself riddled with fungal tunnels) was the typically massive amount of fungus that accumulates as the lesion progresses. Figure 16, from a 12-day-old lesion, is a tangential section

showing a plethora of peripilar arthrospores. Also shown is the marked epidermal hyperplasia which attends development of the lesion.

DISCUSSION

The clarity of detail attained in the micrographs depended on the combination of techniques described. Orientation and architectural relationships were maintained by pinning the biopsy specimens to flat wax blocks before fixa-

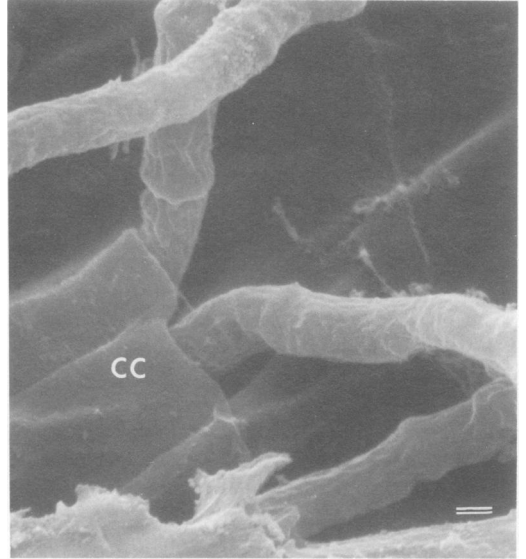


FIG. 9. Hyphal invasion of hair shaft, wedging beneath free edge of cuticular cell (CC). Bar, 0.7 μ m.

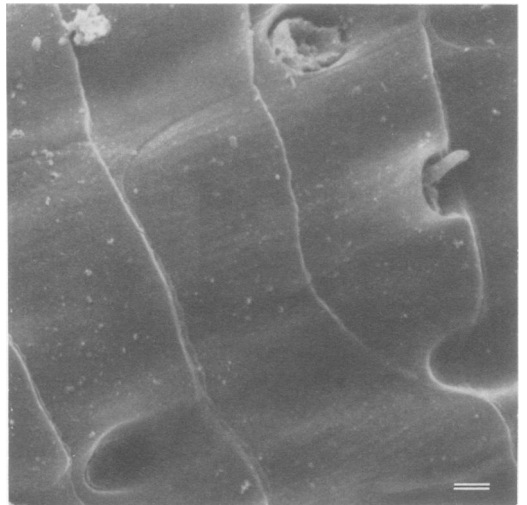


FIG. 10. Hyphal penetration of hair shaft cuticle both in association and not in association with a cuticular cell edge. Bar, 1.0 μ m.

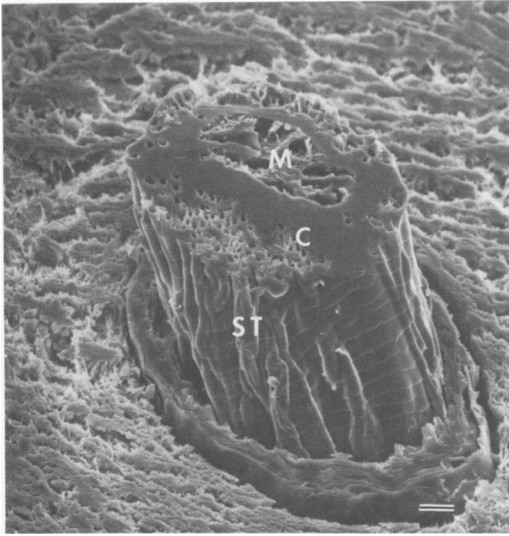


FIG. 11. Hair shaft with varicosities caused by subcuticular hyphal tunneling (ST). Note tunnels also in hair cortex (C). Medullary air spaces (M) are normal. Bar, 7.9 μ m.

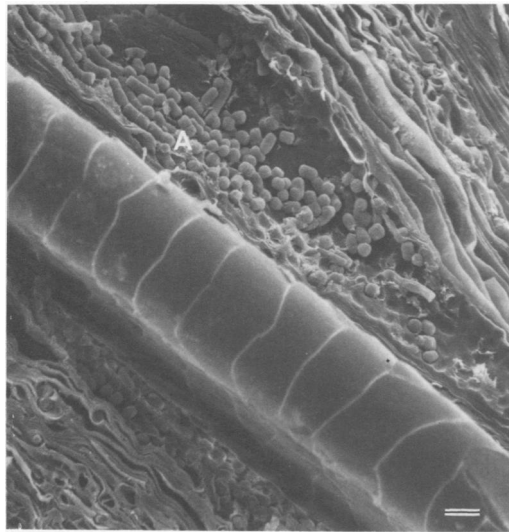


FIG. 12. Arthrospore formation, hyphal fragmentation in progress. Note the cylindrical nature of newly formed arthrospores (A). Bar, 5 μ m.

tion. Also, it was important to fix the tissue before sectioning; when we examined tissues that had been sectioned before fixation, we noted debris, distortion, and poor resolution. We feel that fresh biopsy material gives results superior to paraffin-embedded deparaffinized material and that the critical-point drying technique is essential to avoid further microscopic distortion. Lesions appeared at all inoculation sites by

day 5. Hyphae were first seen by SEM in lesions from day 5. Examination of lesions from consecutive days showed successive involvement of follicles at the lesion's edge. Therefore, various stages of follicular attack could be found in most of the later lesions. Extensive scanning was required to locate enough fortuitously split follicles

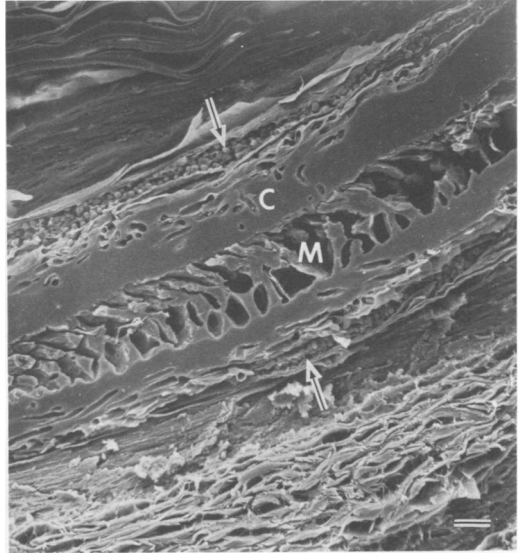


FIG. 13. Arthrospores (arrows) surrounding longitudinally split hair, hyphal tunnels in cortex (C). Medullary air spaces (M) are normal. Bar, 11.5 μ m.



FIG. 14. Predominance of arthrospores (A) in peripilar space. Note sharply twisting, smooth-walled tunnels (arrow) carved by hyphae in hair cortex (C). Bar, 2.1 μ m.

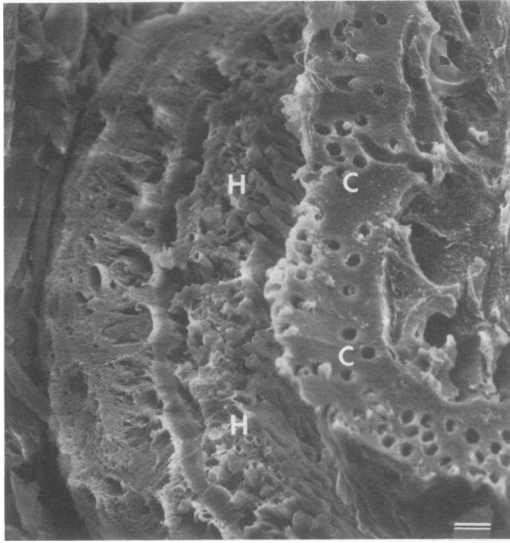


FIG. 15. Cross-sectional view of hyphal mass (H) in the peripilar space. Hair cortex (C) is riddled with fungal tunnels. Bar, 4.7 μ m.

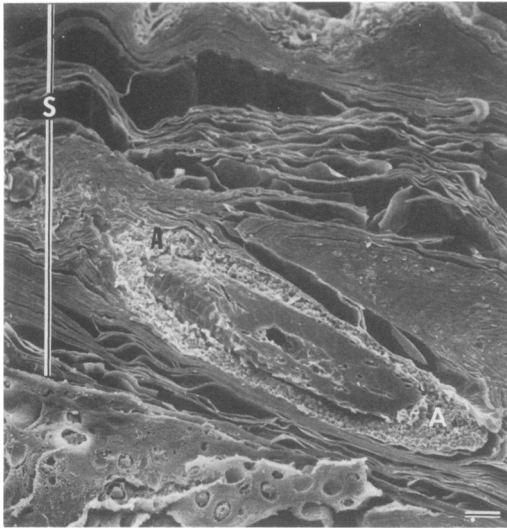


FIG. 16. Tangential section of follicle and shaft showing mass of arthrospores (A) and hyperplastic stratum corneum (S). Bar, 9.4 μ m.

to display the pattern of invasion.

The fungal pathway that we observed did not completely match that described in investigations of human dermatophyte infections. Kligman (6) disputed Sabouraud's (10) widely held view that fungus grows down the follicle, confined within the keratinous lining of the wall. Kligman (6) found instead that the fungi "leave the stratum corneum where the epidermis in-

vaginates to form the follicle and entwine themselves around the hair. They become appressed to it and proliferate on its surface." Our SEM study of guinea pig skin invasion by *T. mentagrophytes* showed that hyphae follow a keratinizing pathway to the lower region of the keratinizing portion of the outer root sheath, where they emerge through the wall to enter the follicular canal (Fig. 3 and 5). Also, hyphae occasionally appear to reenter the wall. In our study, as in another (6), the trend of hyphal growth was obviously downward; upward hyphal orientation was rarely observed (Fig. 3, 5, and 6).

As hyphae grow downward in the peripilar space, they create furrows (Fig. 6, 7, and 8) of various depths on the cuticle of the inner root sheath and on the apposed hair shaft cuticle. Some furrows are so deep in the follicular wall that they appear almost submerged. The relatively shallow impressions in the cuticle of the hair shaft may attest to greater resistance.

We observed fungal penetration of the lower half of the intrafollicular portion of the hair shaft, as previously reported (6). Wedging of hyphae beneath the free edge of cuticular cells, often noted in vitro (1, 2, 4), was commonly seen (Fig. 9). Holes not in association with cuticular cell margins (Fig. 10) were equally common. After penetrating the hair shaft, exuberant hyphal burrowing was evident as tortuous subcuticular varicosities (Fig. 11). Hyphal boring into the hair cortex produced sharply twisting, well-defined, smooth-walled tunnels (Fig. 13 and 14). Fibrillar dissociation of hair cortex appeared much less striking than Tosti et al. (11) had noted in their SEM study of deparaffinized biopsy sections. The present study contains ample morphological evidence to implicate both mechanical pressure and keratin dissolution as invasive mechanisms.

In vivo arthrospore formation (Fig. 12, 13, 14, and 16) appeared similar to that described by Bibel et al. (3) in a recent in vitro SEM study but lacked the described globular material and rings of fibrillar fluff on hyphal surfaces.

More fungus was seen in the follicle than in the stratum corneum. Views of more advanced lesions (Fig. 16) emphasize this disproportionate distribution of fungal mass. One may speculate that the large mass in the follicles may provoke the strong reaction seen in our guinea pig model, which results in temporary alopecia and self-healing of every primary experimental infection.

Scanning electron microscopy of dermatophyte lesion biopsies by techniques described in this report allowed a direct and immediate grasp of how dermatophytes invade. There may be other infectious processes in which the unique

perceptions permitted by SEM can similarly contribute to our understanding of host-parasite relationships.

ACKNOWLEDGMENTS

We thank Roko Smiljanic and Glenda Wilson for technical assistance and Paula Crawford for assistance in manuscript preparation.

LITERATURE CITED

1. **Barlow, A. J. E., and F. W. Chattaway.** 1955. Attack of chemically modified keratin by certain dermatophytes. *J. Invest. Dermatol.* **24**:65-74.
2. **Baxter, M., and P. R. Mann.** 1969. Electron microscopic studies of the invasion of human hair in vitro by three keratinophilic fungi. *Sabouraudia* **7**:33-37.
3. **Bibel, D. J., D. A. Crumrine, K. Yee, and R. D. King.** 1977. Development of arthrospores of *Trichophyton mentagrophytes*. *Infect. Immun.* **15**:958-971.
4. **English, M. P.** 1968. The developmental morphology of the perforation organs and eroding mycelium of dermatophytes. *Sabouraudia* **6**:218-227.
5. **Glauert, A. M.** 1975. Fixation, dehydration and embedding of biological specimens. North Holland Publishing Co., Amsterdam.
6. **Kligman, A. M.** 1955. Tinea capitis due to *Microsporum audouini* and *Microsporum canis*. *Arch. Dermatol.* **71**:313-337.
7. **Montagna, W., and P. F. Parakkal.** 1974. The structure and function of skin. Academic Press Inc., New York.
8. **Pillsbury, D. M., W. B. Shelly, and A. M. Kligman.** 1956. *Dermatology*. The W. B. Saunders Co., Philadelphia.
9. **Reinhardt, J. H., A. M. Allen, D. Gunnison, and W. A. Akers.** 1974. Experimental human *Trichophyton mentagrophytes* infections. *J. Invest. Dermatol.* **63**:419-422.
10. **Sabouraud, R.** 1910. *Les teignes*. Masson, Paris.
11. **Tosti, A., S. Villardita, M. L. Fazzini, and R. Scalici.** 1970. Contribution to the knowledge of dermatophyte invasion of hair. An investigation with the scanning electron microscope. *J. Invest. Dermatol.* **55**:123-134.